NASA Technical Memorandum 110276

An Interactive Software for Conceptual Wing Flutter Analysis and Parametric Study

Vivek Mukhopadhyay
Langley Research Center, Hampton, Virginia

August 1996

National Aeronautics and
Space Administration
Langley Research Center
Hampton, Virginia 23681-0001

AN INTERACTIVE SOFTWARE FOR CONCEPTUAL WING FLUTTER ANALYSIS AND PARAMETRIC STUDY

Vivek Mukhopadhyay*
Systems Analysis Branch,
Aeronautical Systems Analysis Division
MS 248, NASA Langley Research Center

Abstract

An interactive computer program was developed for wing flutter analysis in the conceptual design stage. The objective was to estimate the flutter instability boundary of a flexible cantilever wing, when well defined structural and aerodynamic data are not available, and then study the effect of change in Mach number, dynamic pressure, torsional frequency, sweep, mass ratio, aspect ratio, taper ratio, center of gravity, and pitch inertia, to guide the development of the concept. The software was developed for Macintosh or IBM compatible personal computers, on MathCad application software with integrated documentation, graphics, database and symbolic mathematics. The analysis method was based on non-dimensional parametric plots of two primary flutter parameters, namely Regier number and Flutter number, with normalization factors based on torsional stiffness, sweep, mass ratio, taper ratio, aspect ratio, center of gravity location and pitch inertia radius of gyration. The parametric plots were compiled in a Vought Corporation report from a vast database of past experiments and wind tunnel tests. The computer program was utilized for flutter analysis of the outer wing of a Blended Wing Body concept, proposed by McDonnell Douglas Corporation. Using a set of assumed data, preliminary flutter boundary and flutter dynamic pressure variation with altitude, Mach number and torsional stiffness were determined.

1. Introduction

During an airplane conceptual design stage, it is often necessary to obtain initial estimates of the wing or tail flutter instability boundary, when only the basic planform is known, and much of the structural data, frequency, mass and inertia properties are yet to be established. It is also very useful to conduct a parametric study to determine the effect of change in Mach number, dynamic pressure, torsional frequency, wing sweepback angle, mass ratio, aspect ratio, taper ratio, center of gravity, and pitch moment of inertia, on flutter instability boundary. In order to meet these objectives, an interactive computer program was developed for preliminary flutter analysis of a flexible cantilever wing. The computer program was developed using MathCad[1] application software for Macintosh or IBM compatible personal computers. MathCad has integrated documentation, graphics, database and symbolic mathematics and is well suited for rapid interactive empirical analysis. The current flutter analysis method is based on an experimental database and non-dimensional parametric plots of two primary flutter parameters, namely normalized Regier number and Flutter number, and their variation with Mach number, with normalization factors based on wing geometry, torsional stiffness, sweep, mass ratio, taper ratio, aspect ratio, center of gravity position and pitch inertia radius of gyration. The analysis database and parametric plots were compiled in a Vought Corporation report by Harris[2] from a large number of wind-tunnel flutter model test data. The Regier number is a stiffness-altitude parameter, first studied by Regier[3] for scaled dynamic flutter models. An extension to the use of the Regier number as a flutter design parameter was presented by Frueh[4]. In a recent paper by Dunn[5], Regier number was used to impose flutter constraints on the structural design and optimization of an ideal wing.

The general assumptions, data requirements and interactive analysis procedure were described first. Important non-dimensional plots used for the analysis, along with an example to estimate the flutter boundary and stiffness requirements of the outer wing of a blended wing-body concept[6] were presented. Assuming a set of initial data, preliminary flutter boundary and flutter dynamic pressure variation with Mach number and root-chord torsional stiffness were determined.

2. Nomenclature

AR	aspect ratio based on half wing
a	speed of sound
a_eq	equivalent airspeed = $a/\sqrt{\sigma}$
a0	speed of sound at sea level
C_75	wing chord at 75% semispan
C_60	chord at 60% semispan
cg	wing section center of gravity
CGR	cg location at 60% chord
CR	effective root chord of wing

---

* Systems Analysis Branch, NASA Langley

CT wing tip chord length
EI section bending stiffness (lb-ft^2)
F Flutter number = M / *R*
F_ normalized Flutter number
g acceleration due to gravity
GJ_root wing root torsional stiffness (lb-ft^2)
GJ_mid mid-span torsional stiffness
Ka torsional frequency factor
K_all total correction factor
K_Ar aspect ratio correction factor
K_cg center of gravity correction factor
Kf_ root flexibility correction factor
K_λ taper ratio correction factor
K_μ mass ratio correction factor
K_Rgyb radius of gyration ratio factor
I_60 wing pitch inertia at 60% span (lb-ft^2)
L effective beam length (semispan/cos Λ)
M Mach number
MAC mean aerodynamic chord
MGC mean geometric chord
q dynamic pressure
R surface Regier number
R Regier number
R_ normalized Regier number
R_{gyb} radius of gyration ratio
S effective semispan
V flight velocity (ft/sec)
V_eq equivalent flight velocity = $V\sqrt{\sigma}$
V_R surface Regier velocity index
W_ex weight of exposed wing (lb)
c_hinge elastic axis location
Λ wing sweep back angle
λ wing taper ratio
μ wing mass ratio
μ0 mass ratio at sea level
ρ air density
ρ0 air density at sea level
σ air density ratio ρ/ρ0
ω_α wing torsional frequency
ω_h wing bending frequency

Symbol subscript extensions
_avr average plot
_env envelope plot
_eq equivalent air speed
_KT velocity in Knots
_ls low sweep (0<Λ<20 deg)
_ms moderate sweep (20<Λ<40 deg)
_mid value at mid-span
_root value at wing root

3. General Assumptions

The flutter analysis software is applicable for a conventional cantilevered wing or tail with straight leading and trailing edge as shown in Fig. 1. The primary geometric input data required are root-chord CR, tip-chord CT, effective semispan S, sweep at quarter chord Λ, chordwise location of wing section center of gravity at 60% semispan and location of elastic axis or hingeline for all pitching surface at root chord. The lifting surface of the wing is assumed to be rigidly clamped at an effective root station, and has conventional bending torsional type flutter characteristics. If this effective root is considered to be restrained with a spring, a correction factor is computed and applied to account for the effect of bending and torsional flexibility at this wing station. This feature is useful for an all moving tail surface mounted on a flexible rod or for a blended wing-body type structure where the outer span of the wing is more flexible and primarily contributes to flutter instability and the inner part is relatively rigid. Then the spanwise station of the flexible outer wing is used as effective root station and a correction factor is applied to account for the bending freedom.

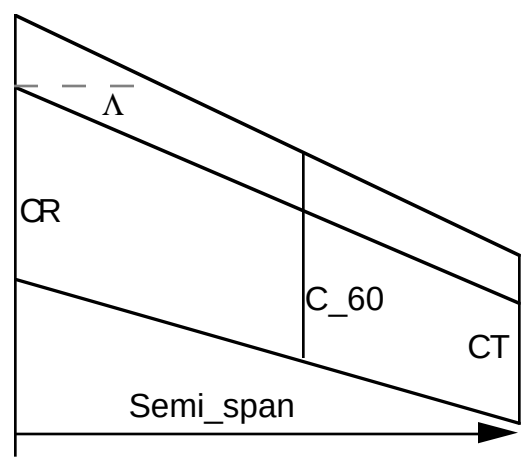

Fig. 1. Conventional wing planform geometry definition for flutter analysis.

The interactive analysis starts with specifying the geometric data and the critical design input parameters. These numerical data can be assigned or changed interactively on the computer screen, for all the parameters which are followed by the assignment symbol :=, and are marked as INPUT. At a later stage, for parametric study, a series of values can also be assigned directly. The rest of the analysis equations, related data and functions are automatically calculated, and all data are plotted to reflect the effect of the new input parameters. The units are also checked for compatibility and converted to the database units before calculations are performed. A typical interactive data input screen is shown in Fig. 2 The primary input data required are root-chord CR, tip-chord CT, effective semispan S, sweep at quarter chord Λ, running pitch moment of inertia I_60 and running weight W_60, both at 60% effective semispan, chordwise location of center of gravity line CGR at 60% semispan as fraction of mean geometric chord

INPUT Root and Tip chord:	$CR := 35.4 \cdot ft$	$CT := 14.5 \cdot ft$	$\lambda := \frac{CT}{CR}$
INPUT effective SEMISPAN:	$Semi\_span := 106.8 \cdot ft$		$\lambda = 0.41$
DefineEffective Aspect ratio: (ONE SIDE ONLY)	$AR := \frac{Semi\_span}{0.5 \cdot (CR + CT)}$		$AR = 4.281$
INPUT Torsional Stiffness at effective root, GJ_root and midspan, along and normal to elastic axis:			
	$GJ\_root := 40 \cdot 10^8 \cdot lb \cdot ft^2$	$GJ\_mid := 24 \cdot 10^8 \cdot lb \cdot ft^2$	$GJ\_Ratio := \frac{GJ\_mid}{GJ\_root}$
INPUT Mach number and Altitude (in 1000 ft):	$Mach := 0.6$	$Alt := 0$	
INPUT Sweep angle at quarter chord	$\Lambda := 37 \cdot deg$		
INPUT WEIGHT DATA:			
Pitch axis moment of inertia: I_pitch	$I\_pitch := 7.0 \cdot 10^5 \cdot lb \cdot ft^2$		
Running Pitch moment of inertia at 60% Semi Span: I_60	$I\_60 := 16000 \cdot \left(\frac{lb \cdot ft^2}{ft}\right)$		
Running weight at 60% of exposed Span station: W_60	$W\_60 := 500 \cdot \frac{lb}{ft}$		
INPUT CG Location at 60% as fraction of MGC chord: CGR	$CGR := 0.45$	$MGC := \frac{2}{3} \cdot \left(\frac{1 + \lambda + \lambda^2}{1 + \lambda}\right) \cdot CR$	
INPUT Exposed weight per side W_ex	$W\_ex := 6.69 \cdot 10^4 \cdot lb$	$MGC = 26.409 \cdot ft$	

Fig.2 Interactive INPUT screen for geometry, stiffness, Mach number, altitude, weight and pitch inertia data.

and total weight of the exposed surface W_ex. Fig. 2 also shows symbolic computation of taper ratio, aspect ratio, stiffness ratio and mean geometric chord of semispan. Structural data required are torsional stiffness at wing root GJ_root and at mid-span GJ_mid from which first torsional frequency ω_α is computed. If available, primary bending and torsional frequencies may be supplied instead. Additional input required are location of elastic axis or hingeline for all moving surface and the ratio of primary torsion over bending frequencies. Also required are the reference flutter critical flight altitude and Mach number which are generally chosen at sea level and at maximum design dive speed, respectively. The input data set is used to compute the torsion frequency and the two basic flutter indexes, namely Regier number and Flutter number which are described next.

4. Regier number and Flutter number

The first step in the analysis process is to compute the all important non dimensional parameter called surface Regier number R and surface Regier velocity index V_R of the wing, which are defined at sea level as

Regier_no $R := V\_R / a0$ (1)

where

$$V\_R = 0.5 C\_75 \omega_\alpha \sqrt{\mu 0} \quad (2)$$

The surface Regier number can be interpreted as a ratio of elastic force over aerodynamic force at sea level. Although V_R is actually a stiffness parameter proportional to the wing uncoupled torsional frequency ω_α, and is called surface flutter parameter in the original report[2], it is referred to as surface Regier velocity index in this paper, since it has the unit of velocity. The Regier surface velocity index V_R is also defined as a function denoted by v_R(GJ_Ratio, GJ_root, I_60, L, C_75, μ0). During the conceptual design stage, detailed structural data are generally not available for computing the wing uncoupled torsional frequency ω_α, hence an empirical formula[2] based on a torsional frequency factor Ka is used, as shown in Eq.(3) in radians/second unit.

$$\omega_\alpha = \frac{Ka}{L}\sqrt{\frac{GJ\_root}{I\_60 / g}} \qquad (3)$$

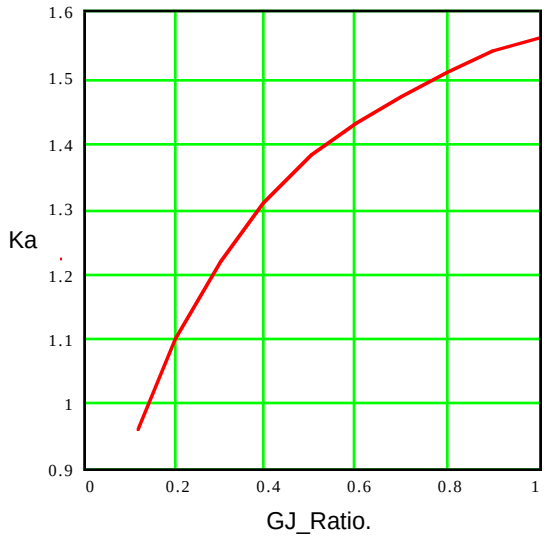

Fig. 3. Interpolated plot of factor Ka as a function of GJ_Ratio for estimating torsional frequency.

Fig. 3 shows the plot of the factor Ka as a function of GJ_Ratio, which is defined by torsional stiffness GJ at midwing divided by GJ_root. The original plot was compiled[2] by computing Ka from numerous experimental data and then drawing a mean line through the data. Using the computed GJ_Ratio, the factor Ka is automatically calculated from Fig. 3 using a linear interpolation function, and is then used to compute the torsional frequency ω_α from Eq.(3). If a detailed finite element model of the wing is available for vibration frequency analysis, a better estimate of the torsional frequency ω_α can be used instead.

The second important non dimensional parameter called Flutter number *F* is defined as equivalent air speed at sea level V_eq divided by surface Regier velocity index *V_R* as shown in Eq.(4). Note that Regier number *R* and Flutter number *F* are inversely proportional and satisfy Eq.(5). The Flutter number corresponding to the equivalent flutter velocity is determined from a set of non dimensional plots as described next and is compared with the actual flutter number in order to determine the flutter velocity safety margin, which should be above 20% at sea level maximum dive speed.

$$\text{Flutter\_no}\ \ F := \text{V\_eq} / V\_R \qquad (4)$$

$$\text{Flutter\_no}\ \ F := \text{M} / \text{Regier\_no} \qquad (5)$$

5. Flutter Boundary Estimation

The second step in the basic flutter analysis process are described in this section. The analysis uses a set of experimental data plots compiled by Harris[2]. Only those plots which are applicable to a conventional straight leading and trailing edge planform wing with moderate sweep between 20 and 40 degrees, are presented in this section and in Appendix A. The corresponding plots applicable to a conventional planform wing with low sweep between 0 and 20 degrees are presented in Appendix B. Additional data for flutter analysis of highly swept and delta wing are available in Ref. 2.

The flutter analysis is accomplished by using two basic normalized flutter index plots, namely Regier number and Flutter number as a function of Mach number as shown in Figs. 4 and 5. These plots were based on experimental and analytical flutter studies of these two flutter indexes which were normalized by nominal values of five basic parameters, namely sea level mass ratio, taper ratio, aspect ratio, chordwise center of gravity position, and pitching radius of gyration. The original plots also include the normal values of these parameters, and their range for which these plots are valid. The plot of these two normalized flutter indexes computed from a large number of experimental data are also shown in the original report[2]. In the computer program, only the essential data for medium and low sweep wings are stored and used using an automatic interpolation and data retrieval capability.

Figure 4 shows the flutter boundary estimation diagram of normalized Regier number versus Mach number, for conventional planform, moderate sweep wings. The first plot shows upper limits of the Regier number versus Mach number for normal values of the key basic parameters, i.e. mass ratio of 30, taper ratio of 0.6, aspect ratio of 2 and radius of gyration ratio Rgyb_60 of 0.5. The solid line is a conservative upper limit envelope and is denoted by R_ms_env(M). The lower dashed line is an average non conservative upper limit denoted by R_ms_avr(M). These two plots were compiled[2] by computing the normalized Regier number from numerous experimental data and then drawing an upper bound and a mean line through the data points. If the normalized Regier number of the wing being designed is greater than the upper bound plot over the Mach number range, then the wing is considered flutter free at the specified Mach number. If the normalized Regier number falls in between the two plots then the wing may be marginally stable. If it falls below, the wing may be unstable and would require further analysis and design.

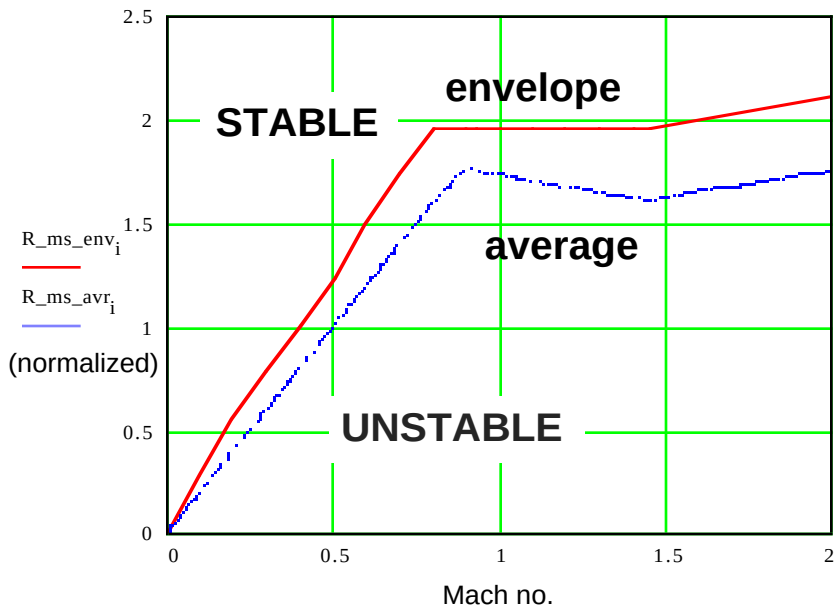

Fig. 4. Flutter boundary estimation diagram of normalized Regier number versus Mach number M for moderate sweep wings (20<Λ<40 degrees).

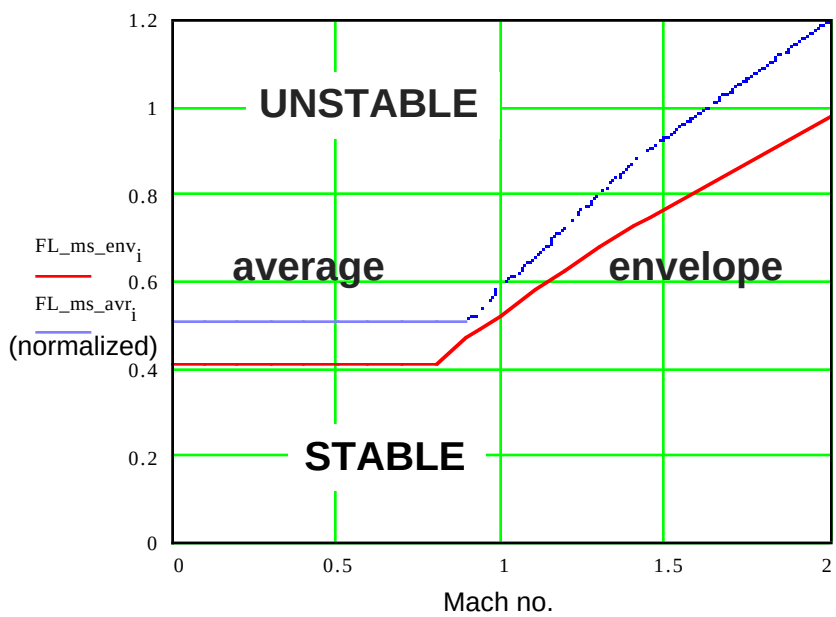

Fig. 5. Flutter boundary diagram estimation diagram of normalized Flutter number versus Mach number M for moderate sweet wings (20<Λ<40 degrees).

Figure 5 shows the flutter boundary estimation diagram of the Flutter number versus Mach number, for a conventional planform, moderate sweep wing. This plot is also used to estimate the equivalent flutter velocity and flutter dynamic pressure. In this figure the solid line is a conservative lower limit envelope and is denoted by FL_ms_env(M). The dotted line is an average non conservative lower limit flutter boundary and is denoted by FL_ms_avr(M). If the normalized Flutter number of the wing being designed is smaller than the lower bound denoted by the solid line over the Mach number range, then the wing is considered to be flutter free at the specified Mach number at sea level. If the normalized Flutter number falls in between the solid and dotted line boundaries then the wing may be marginally stable. If the Flutter

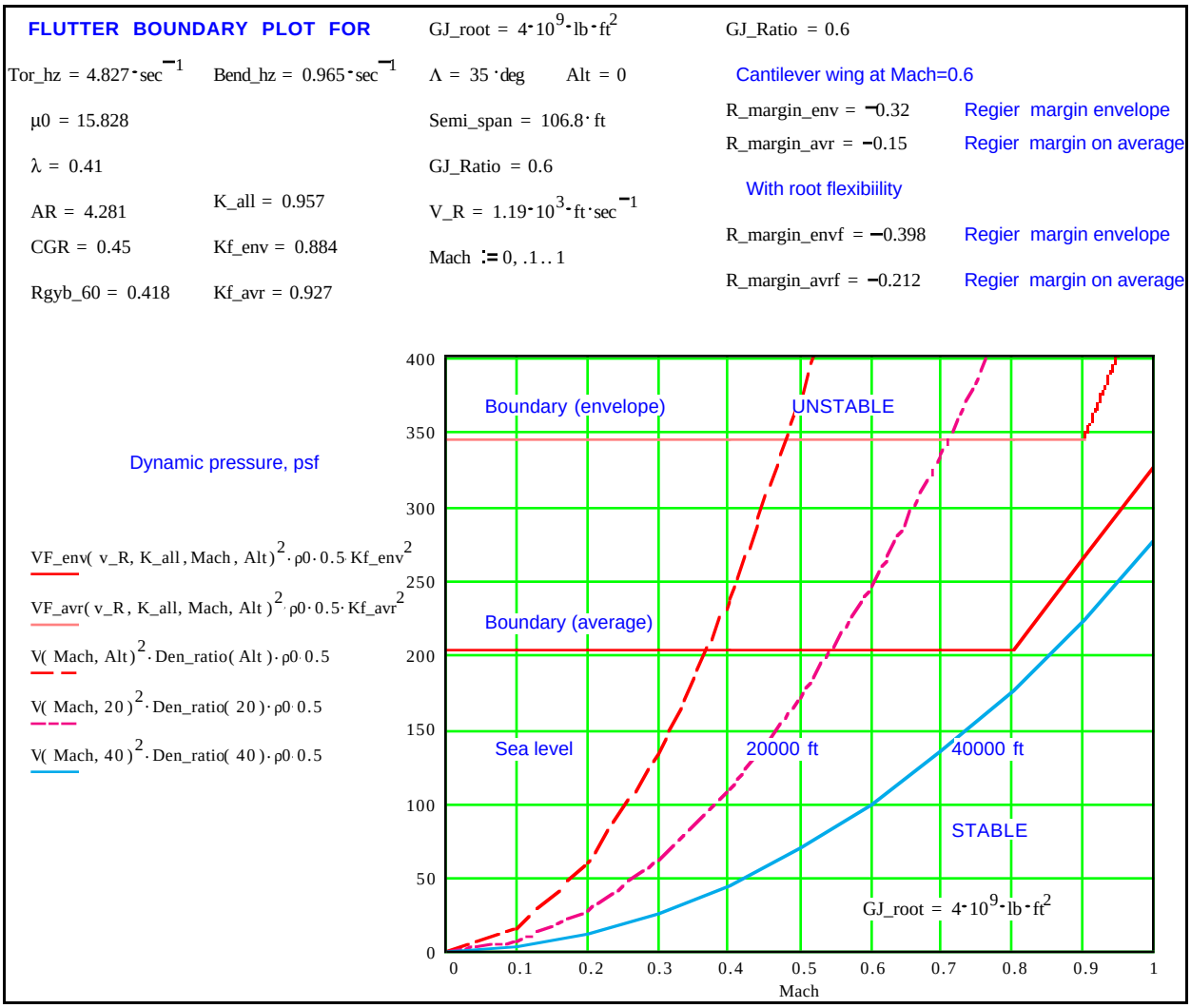

Fig. 6. Summary of interactive flutter analysis results and flutter dynamic pressure boundary plot as they appear on the computer screen.

number is above the dotted line boundary, the wing may be unstable in flutter.

Since Figs. 4 and 5 are based on normalized Regier number and Flutter number, the actual Regier number is determined by <u>dividing</u> R_ms_env(M) and R_ms_avr(M) by a total correction factor K_all, to account for actual values of the five key parameters, namely mass ratio μ0, taper ratio λ, aspect ratio AR, center of gravity ratio CGR and pitch radius of gyration ratio at 60% semispan Rgyb_60 as shown in Eq.6. Since the Flutter number is Mach number over Regier number, the actual Flutter number is determined by <u>multiplying</u> FL_ms_env(M) and FL_ms_avr(M) by the total correction factor K_all as shown in Eq.7. This total correction factor K_all is a product of all the five key parameter correction factors for mass ratio k_μm(μ0), taper ratio K_λ, aspect ratio K_Ar(Ar), CG position ratio K_CG(CGR) and radius of gyration ratio K_Rgyb(Rgyb_60) as shown in Eq.8. The relationship between these five key parameters and the corresponding correction factors for moderate sweep wings and plots used to determine these correction factors are presented in Appendix A, to provide some insight into their effect on flutter boundary. The corresponding plots for low sweep wings are presented in Appendix B.

The computer program automatically computes K_all and applies this overall correction factor to the normalized stability envelopes R_ms_env(M) and FL_ms_env(M), at the reference Mach number M at sea level, using the relations,

Regier_env(M) := R_ms_env(M) / K_all (6)

Flutter_env(M) := FL_ms_env(M) x K_all (7)

where total correction factor K_all is defined as the product

K_all := K_μm(μ0). K_λ(λ) K_Ar(Ar).
K_CG(CGR). K_Rgyb(Rgyb_60). (8)

The overall correction factor K_all is also applied to the normalized average stability bounds R_ms_avr(M) and F_ms_avr(M) in a similar manner. Thus a correction factor greater than unity is beneficial to flutter stability.

If this effective root is considered to be flexible, additional correction factors Kf_env and Kf_avr are computed and applied to account for the effect of bending and torsional flexibility at this wing station. Additional input required for this correction factor are chordwise location of elastic axis line c_hinge at root chord and the ratio of torsion or pitch frequency over bending or heave frequency fp/fh. The flexibility correction factors Kf_env and Kf_avr are determined using the parametric plots shown in Appendix C. Then each factor is multiplied by K_all from Eq.(8) and are used to modify the Regier_env(M), Regier_avr(M), Flutter_env(M) and Flutter_avr(M) as shown in Eqs.(6) and (7).

After all the correction factors are applied to the flutter boundary data from Figs. 4 and 5, actual values of Regier_env(M) and Flutter_env(M) are compared with surface Regier number R and Flutter number F of the specific wing under consideration. Thus at a given Mach number corresponding to the maximum dive speed at sea level, if the computed surface Regier number R and Flutter number F, satisfy the inequalities

R > Regier_env(M) (9)

F < Flutter_env(M) (10)

then the cantilever wing can be considered flutter free at the specified Mach number at sea level. On the other hand, if

Regier_env(M) > R > Regier_avr(M) and

Flutter_env(M) < F < Flutter_avr(M) (11)

then the wing may be marginally stable or unstable and may require redesign or refined analysis. Finally if

R < Regier_avr(M) and

F > Flutter_avr(M) (12)

then the wing can be considered to have unstable flutter characteristics at the specified Mach number at sea level. The computer program automatically makes these comparison, computes the surface Regier velocity margins from the upper envelope and average Regier velocity boundary, estimates the corresponding flutter dynamic pressure boundary and then plots the flutter boundary and flight dynamic pressure versus Mach number at sea level, 20000 feet and 40000 feet altitude as shown in Fig. 6. Figure 6 also shows a summary of all the results along with the flutter boundary plot as they appear in the interactive computer screen. The wing effective root torsional stiffness GJ_root, GJ_Ratio, semispan, sweepback angle Λ, primary torsion and bending frequencies, along with the five key parameters μ0, λ, AR, CGR and Rgyb_60 are shown at top and upper left. The corresponding correction factor K_all along with the flexibility correction factors Kf_env and Kf_avr are shown next. The surface Regier velocity V_R and surface Regier number margins without and with root flexibility correction at Mach 0.6 are shown at upper right. The sea level flutter velocities VF_env and VF_avr are computed by multiplying the corresponding Flutter_env(M) and Flutter_avr(M) by surface Regier velocity V_R. The dynamic pressure quantities being plotted along with legends are shown in the left label.

6. Parametric Study

The initial data and final flutter boundary estimation results shown in Figs 2 and 6 are explained in this section along with a parametric study to estimate outer wing effective root-chord stiffness requirements for a flutter free wing. Figure 7 shows the baseline outer wing planform and value of key parameters of a blended-wing-body transport concept[6]. The outer wing has a semispan of 106.8 feet. The effective root-chord is assumed to have a torsional stiffness of $4x10^9$ lb-ft^2. Using Fig. 3 and the method described in section 4, the torsional frequency is estimated to be 4.2 Hz. The quarter chord sweep is 37 degrees, the sea level mass ratio is 15.8, the aspect ratio based on the outer wing semispan is 4.3, the center of gravity line is assumed to be at 45% chord, and the pitch radius of gyration ratio is assumed to be 0.42. The results presented here include an effective root flexibility correction factor Kf is Kf_env=0.88 and Kf_avr=0.93 .

A parametric study of flutter boundary with change in effective wing-root chord torsional stiffness is presented in Figs. 8 and 9. This is done by assigning an array of values to the torsional stiffness variable GJ_root while keeping all other geometric parameters fixed. The computer program automatically plots the corresponding Regier_number and Flutter_number along with the flutter boundary at the reference Mach number 0.6, at sea level as shown in these figures.

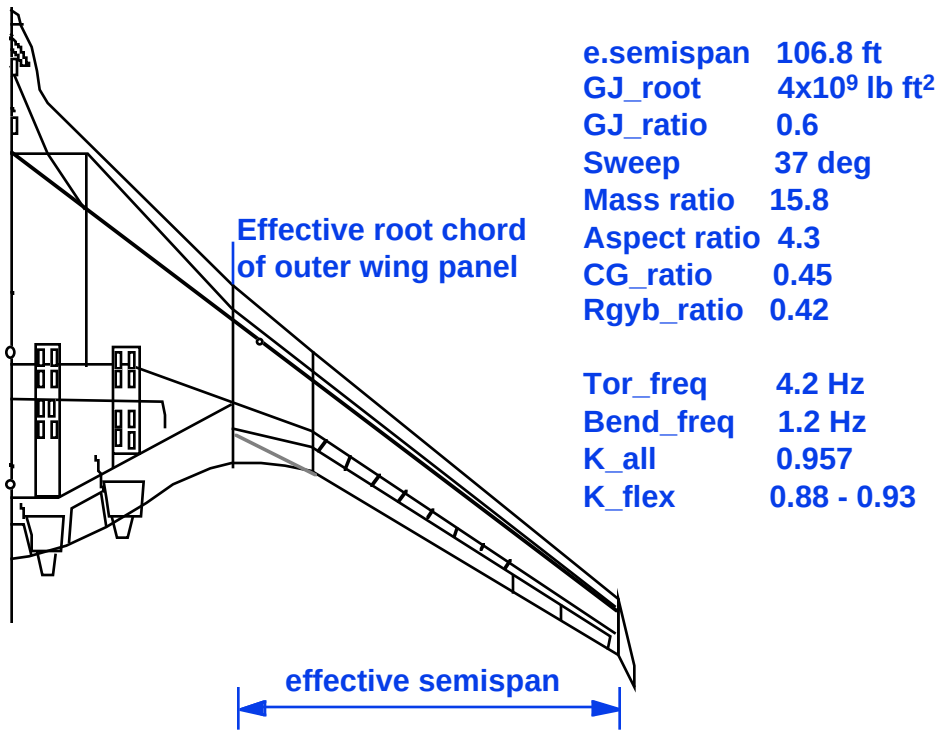

Fig. 7. Geometry and structural data used for flutter analysis of the outer wing panel of a blended wing-body transport concept.

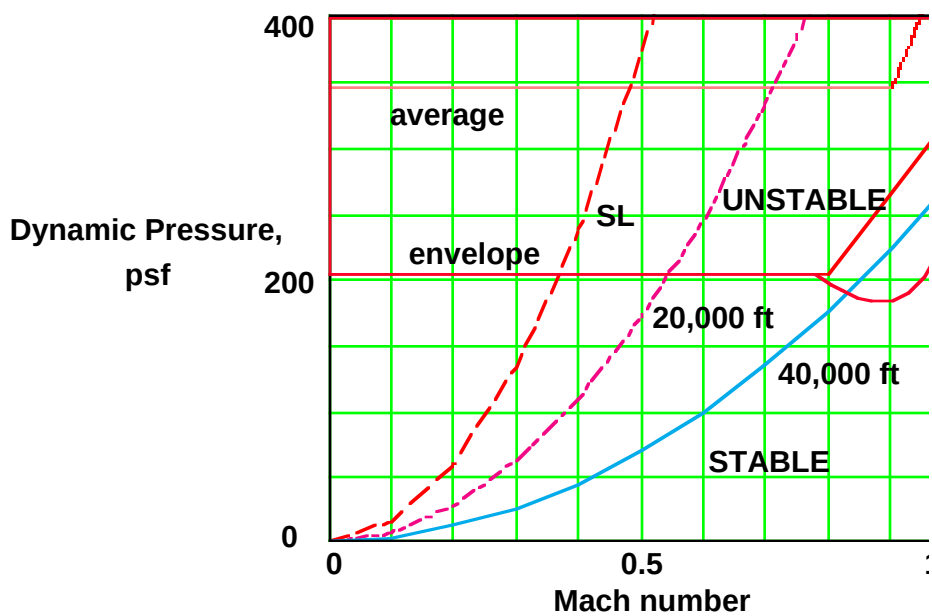

Fig. 8. Outer wing flutter dynamic pressure boundary vs. Mach number for wing-root torsional stiffness 40×10^8 lb-ft^2.

The corresponding Regier velocity index and flutter velocity are also plotted in the computer program, but are not shown here.

Figure 8 shows the initial estimates of the outer wing flutter dynamic pressure boundary versus Mach number for a wing with an effective root-chord torsional stiffness of 4×10^9 lb-ft^2, at sea level, 20000 feet and 40000 feet altitude. This figure indicates that at 40000 feet altitude, the wing would barely clear the flutter boundary at Mach 0.85. However, the wing would still be susceptible to flutter near this cruise

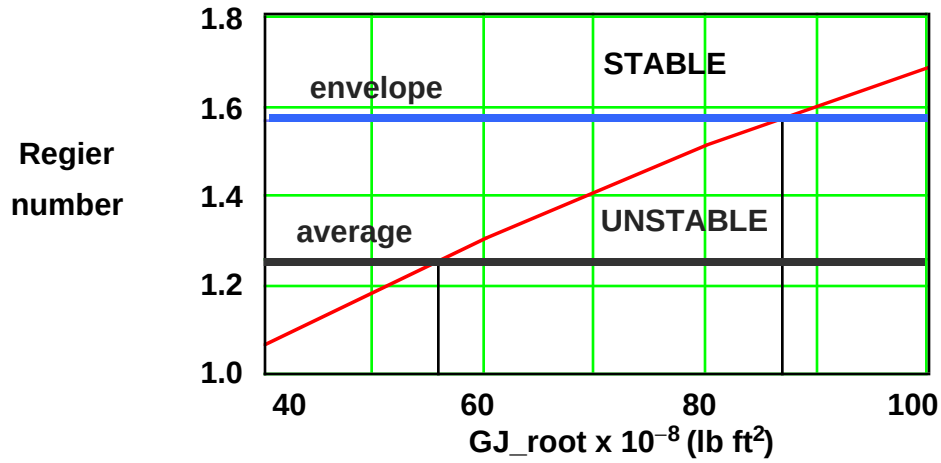

Fig. 9. Variation of surface Regier number with wing root-chord torsional stiffness at a Mach 0.6 at sea level.

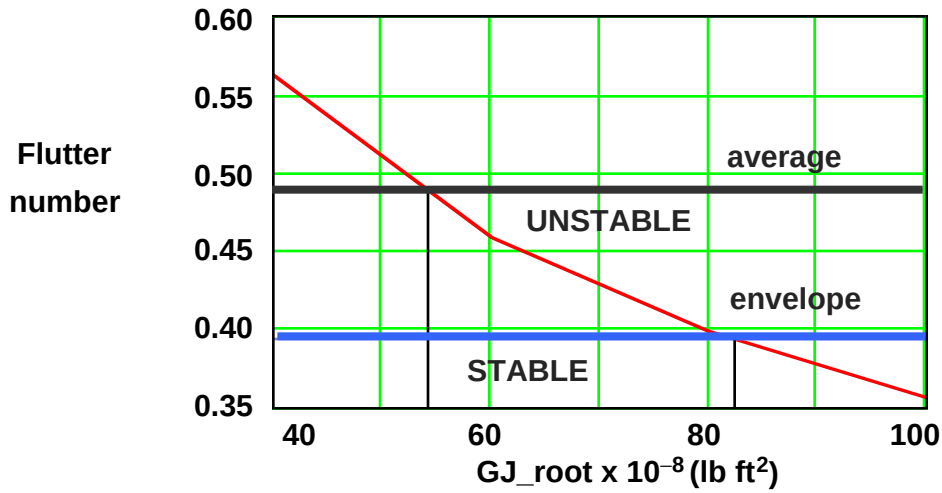

Fig. 10. Flutter number vs. wing root-chord torsional stiffness at Mach 0.6 at sea level.

altitude of 40000 ft and Mach number 0.85, since the flutter dynamic pressure boundary has a dip at this transonic speed as shown in Fig. 8. Hence, detailed transonic flutter analysis would be necessary and the minimum effective wing-root torsional stiffness should be significantly more than 40×10^8 lb-ft^2. A parametric study to estimate an adequate torsional stiffness is described next.

Results of a parametric study to estimate outer wing effective root-chord stiffness requirements for a flutter free wing is shown in Figs. 9 and 10. This exercise demonstrated the versatility and flexibility of this interactive software. First a range of values were assigned to the wing-root stiffness variable GJ_root. The corresponding Regier numbers and Flutter numbers along with the 'average' and 'envelope' stability boundaries were plotted. Fig. 9 shows the variation of Regier number with wing root-chord torsional stiffness and the flutter boundaries at a Mach 0.6, at sea level. The two flutter boundaries labeled 'envelope' and 'average' represent an upper bound and a non conservative average flutter stability boundary, respectively[2]. If the Regier number of the wing is greater than the upper boundary of the region labeled 'stable' over the Mach number range, then the wing is considered flutter free.

Figure 10 shows the variation of Flutter number with wing root-chord torsional stiffness. If the Flutter number of the wing is smaller than the lower bound of the region labeled 'stable' over the Mach number range, then the wing is flutter free. Figs. 9 and 10 indicate that conservatively, the wing could have 5% to 10% flutter velocity margin at Mach 0.6 at sea level if the wing effective root-chord torsional stiffness exceeded 100×10^8 lb-ft^2.

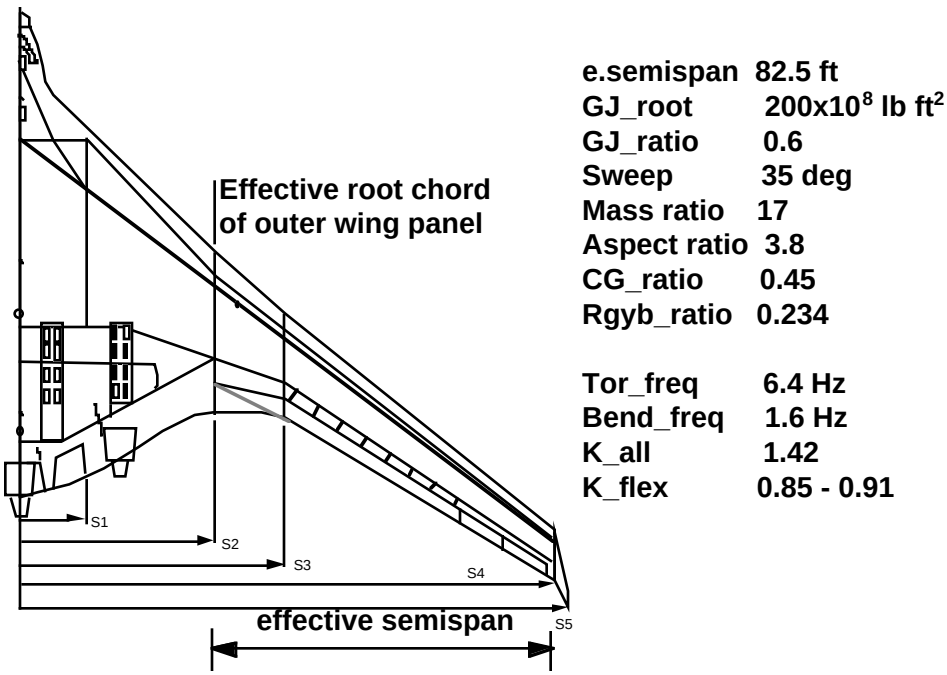

Fig. 11. Geometry and structural data of redesigned wing with reduced span.

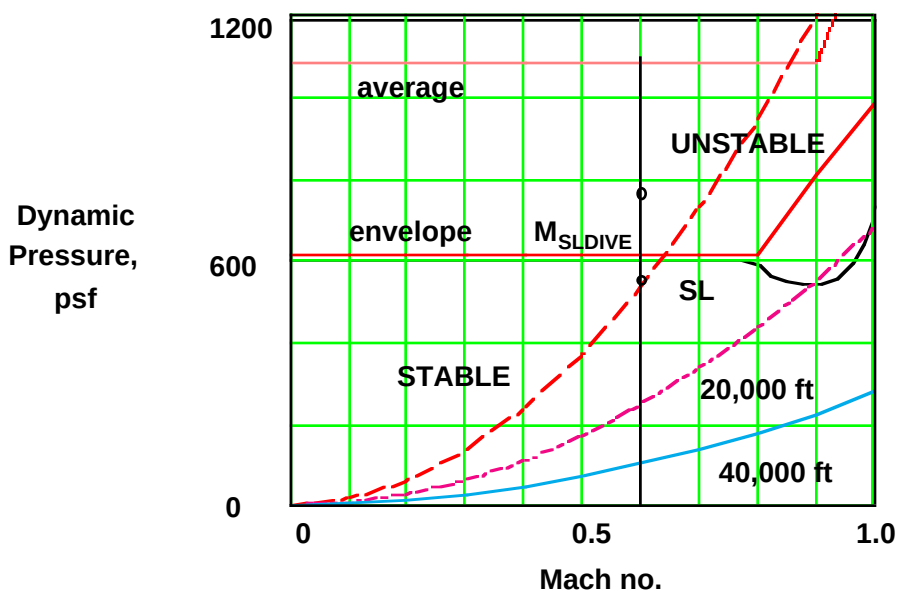

Fig. 12. Reduced span outer wing flutter boundary vs. Mach No. for wing-root torsional stiffness 200×10^8 lb-ft^2.

7. Wing redesign

In these conceptual studies, many of the initial data such as effective wing root torsional stiffness, pitch radius of gyration and effective wing-root flexibility effects were chosen somewhat arbitrarily and the final results were sensitive to these values. However, the answers provided a good indication of flutter problems and stiffness requirements of such large wings. In a subsequent redesign of this proposed airplane[8] based on flight performance and a new propulsion system, the span of the wing was reduced significantly. In this redesign, the effective semispan was estimated to be 82.5 ft. Based on the new wing loading and static structural design[8], the torsional stiffness at the effective wing-root chord station was estimated to be 200×10^8 lb-ft^2. The input data and flutter analysis of this redesigned wing with reduced span are presented in

Figs. 11 and 12. Some of the preliminary results were originally presented in Ref. 9.

Figure 11 indicates that with this reduced span stiffer wing, the estimated torsional frequency is increased to 6.4 Hz from 4.2 Hz. The ratio of torsion to bending frequency fp/fh is assumed to be 4. Although the radius of gyration has decreased, the increased stiffness, mass ratio and reduced aspect ratio resulted in a higher overall correction factor and 300% improvement in flutter boundary dynamic pressure.

Figure 12 shows the flutter boundary of the redesigned wing. At sea level the maximum dive dynamic pressure is 550 psf at Mach 0.6, shown by the first dot on the vertical line in Fig. 12. This flight condition falls below the conservative flutter boundary envelope, and can be considered stable. However, in order to maintain a 20% margin in flutter speed or equivalently 44% margin in flutter dynamic pressure, at maximum dive dynamic pressure, the actual flutter boundary should be above 792 psf, shown by the second dot on this vertical line at Mach 0.6 in Fig. 12. Since the estimated flutter dynamic pressure from the present procedure is between 610 psf and 1080 psf, the main outer wing would marginally satisfy the 44% flutter margin of safety. However, a refined flutter analysis would be required to support this preliminary analysis.

8. Conclusions

An easy to use, interactive computer program for rapid wing flutter analysis was developed on a MathCad platform. The analysis is based on non dimensional parametric plots of Regier number and Flutter number derived from an experimental database and handbook on flutter analysis compiled at Vought Corporation. Using this empirical method, the effects of wing torsional stiffness, sweep angle, mass ratio, aspect ratio, center of gravity location and pitch inertia radius of gyration can be easily analyzed at the conceptual design stage. The entire data and formulae used in the analysis can be displayed on computer screen in graphical and symbolic form. The analysis method was applied to investigate the flutter characteristics of the outer wing of a blended-wing-body transport concept. An Initial set of flutter instability boundaries and flutter dynamic pressure estimates were obtained. A parametric study also established that the effective wing-root chord minimal torsional stiffness should be above 100×10^9 lb-ft^2 for a flutter free wing. In a later cycle of wing static structural design, the torsional stiffness at the effective wing-root chord station was estimated to be 200×10^9 lb-ft^2. Flutter analysis of this redesigned wing indicated that it would marginally satisfy the 44% flutter margin of safety. However, a refined flutter analysis would be required to support this preliminary analysis, if the configuration is further developed.

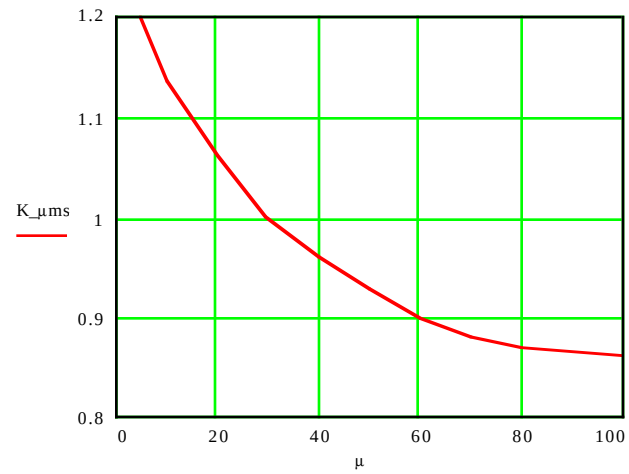

Fig. 13. Sea level mass ratio correction factor K_µms for moderate sweep wing.

APPENDIX A
Correction factors

The relationship between the five key parameters sea level mass ratio µ0, taper ratio λ, aspect ratio AR, CG position ratio CGR and radius of gyration ratio Rgyb_60 and the corresponding correction factors, namely k_µm(µ0), K_λ, K_Ar(Ar), K_CG(CGR) and K_Rgyb(Rgyb_60) in Eq.(8) as discussed in section 5 and plots used to determine these correction factors are presented here. Each correction factor is multiplied and are used to modify the Regier_env(M), Regier_avr(M), Flutter_env(M) and Flutter_avr(M) as shown in Eqs. (6) and (7). Thus a correction factor greater than unity is beneficial to flutter stability.

The sea level mass ratio µ0 is defined as the ratio of mass of the exposed wing and mass of air at sea level in a tapered cylinder enclosing the semispan S with local chord c as its diameter, namely

$$\mu 0 := \frac{W\_ex}{\pi.\rho 0.\int_0^S (c/2)^2\, dy}$$

or

$$\mu 0 := \frac{W\_ex}{\pi.\rho 0.(1+\lambda+\lambda^2).CR^2.S/12}$$

for a straight edge wing, where λ is the taper ratio, CR is root chord and ρ0 is the standard sea level air density 2116.23 lb/ft^2. The correction factor K_µms versus mass ration µ plot (normalized mass ratio 30) for a medium sweep wing is shown in Fig. 13. The plot indicates that increased mass ratio decreases flutter stability margin since, a lower correction factor decreases the flutter boundary envelope Flutter_env(M)

as indicated in Eq.(7). The physical reason is that the increased mass ratio represents reduction in torsional frequency.

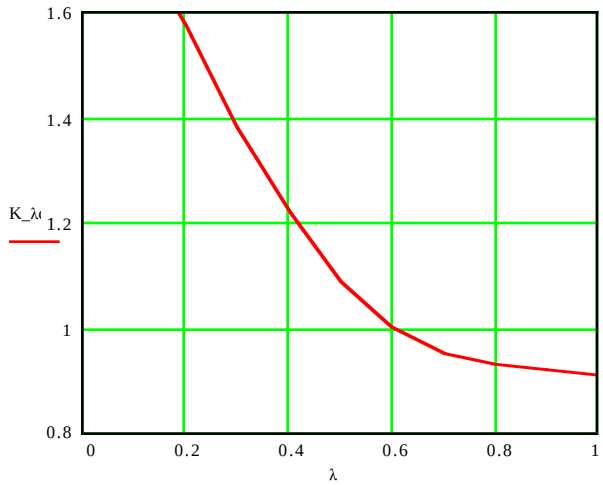

Fig. 14 Taper ratio correction factor K_λ .

The plot for determining the correction factor K_λ for taper ratio is shown in Fig. 14, which indicates that increased taper ratio would decrease flutter stability margin in general, due to decreased Flutter_env(M) as indicated by Eq.(7). The reduction in margin is more pronounced for taper ratios less that 0.6. Physically this is due to increased wing outboard flexibility

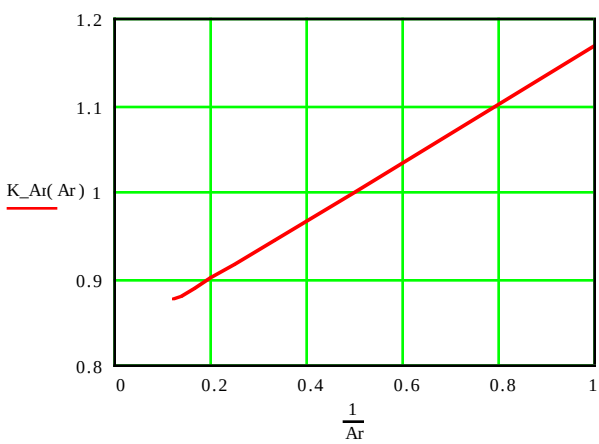

Fig. 15 Aspect ratio correction factor K_Ar vs. 1/Ar.

The plot for determining the correction factor K_Ar for aspect ratio is shown in Fig. 15, which indicates that increased aspect ratio would decrease flutter stability margin. This relation can be approximated as

$$K\_Ar(Ar) := 1 + \frac{5}{15}\cdot\left(\frac{1}{Ar} - 0.5\right)$$

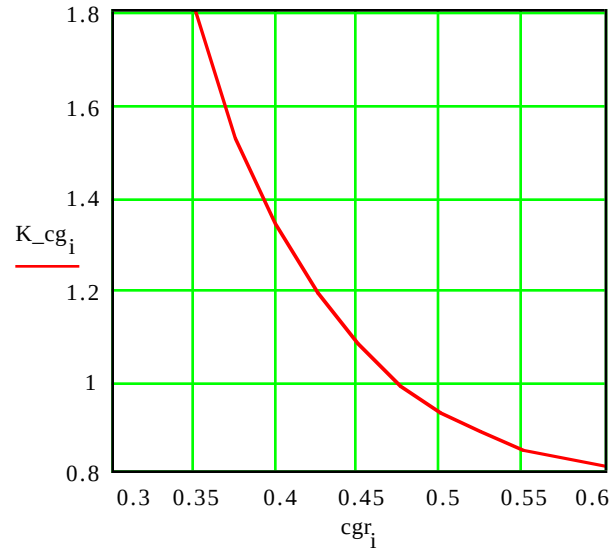

Fig. 16 Center of gravity correction factor K_cg.

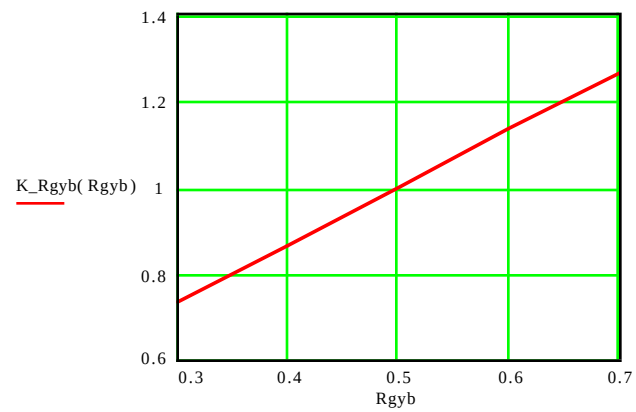

Fig. 17 Radius of gyration ratio correction factor K_Rgyb.

The plot for determining the correction factor K_cg for chordwise position of center of gravity is shown in Fig. 16, which indicates that rearward movement of CG would decrease flutter stability, due to reduced pitch inertia. The wing mounted engines have forward overhang to move the overall CG forward. Fig. 17 shows the plot for determining correction factor K_Rgyb versus radius of gyration ratio at 60% semispan defined as

$$Rgyb\_60 = \frac{2}{C\_60}\sqrt{\frac{I\_60}{W\_60}}$$

This figure indicates that increased radius of gyration has beneficial effect on flutter stability margin, due to increased pitch inertia.

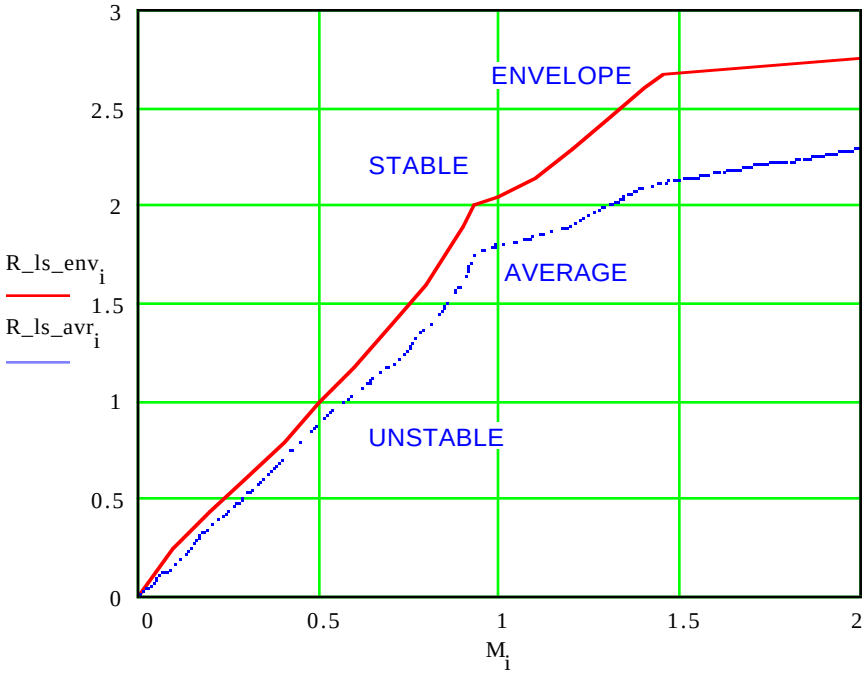

Fig. 18. Flutter boundary estimation diagram of normalized Regier number versus Mach number M for low swept wings (0<Λ<20 degrees).

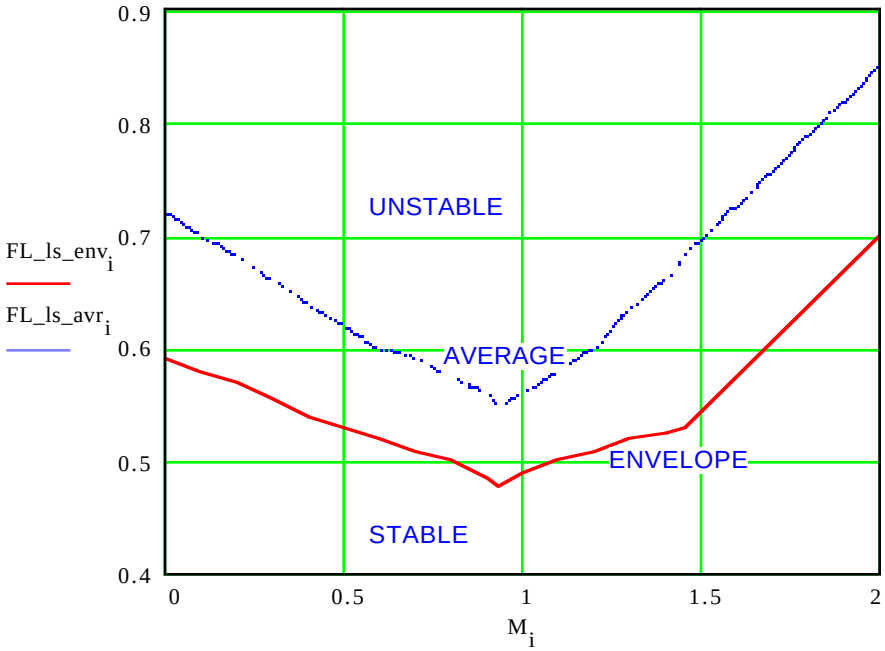

Fig. 19. Flutter boundary estimation diagram of normalized Flutter number versus Mach number M for low swept wings (0<Λ<20 degrees).

APPENDIX B
Low sweep wing analysis.

Flutter boundary estimation diagrams of normalized Regier number and Flutter number versus Mach number M for low swept wings (0<Λ<20 degrees) are presented here. Figure 18 shows the flutter boundary estimation diagram of normalized Regier number versus Mach number, for conventional planform, low swept wings. The plot shows upper limits of the Regier number versus Mach number for normal values of the key basic parameters, i.e. mass ratio of 30,

taper ratio of 0.6, aspect ratio of 2 and radius of gyration ratio Rgyb_60 of 0.5. The solid line is a conservative upper limit envelope and is denoted by R_ls_env(M). The lower dashed line is an average non conservative upper limit denoted by R_ls_avr(M). These two plots were compiled[2] by computing the normalized Regier number from numerous experimental data and then drawing an upper bound and a mean line through the data points. If the normalized Regier number of the wing being designed is greater than the upper bound plot over the Mach number range, then the wing is considered flutter free. If the normalized Regier number falls in between the two plots then the wing may be marginally stable. If it falls below, the wing may be unstable and would require further analysis and design.

Figure 19 shows the flutter boundary estimation diagram of the Flutter number versus Mach number, for a conventional planform, low sweep wing. This plot is used to estimate the equivalent flutter velocity and flutter dynamic pressure. In Fig. 19 the solid line is a conservative lower limit envelope and is denoted by F_ls_env(M). The dotted line is an average non conservative lower limit flutter boundary and is denoted by F_ls_avr(M). If the normalized Flutter number of the wing being designed is smaller than the lower bound denoted by the solid line over the Mach number range, then the wing is considered to be flutter free. If the normalized Flutter number falls in between the solid and dotted line boundaries then the wing may be marginally stable. If the Flutter number is above the dotted line boundary, the wing may be unstable in flutter.

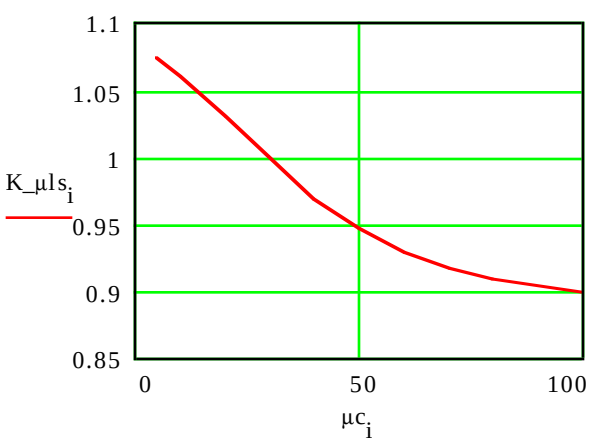

Fig. 20. Sea level mass ratio correction factor K_µls for low sweep wing (0<Λ<20 degrees).

The relationship between the key parameters sea level mass ratio µ0, and the corresponding correction factor k_µls(µ0) for low swept wing and plot used to determine these correction factors is presented in Fig. 20. For other correction factors use those in Appendix A. The correction factor K_µls(µ0) vs. sea level mass ratio plot (normalized mass ratio 30) for low sweep wing in Fig. 20 indicates that increased mass ratio decreases flutter stability margin since, a lower correction factor decreases the flutter boundary envelope Flutter_env(M) as indicated in Eq.(7).

Appendix C
Flexibility correction factors

Correction factors Kf_env and Kf_avr are computed and applied to account for the effect of bending and torsional flexibility at this wing station. Additional input required for this correction factor are chordwise location of elastic axis line c_hinge at root chord as a ratio of mean geometric chord and the ratio of pitch frequency over bending or heave frequency fp/fh. The flexibility correction factors for the envelope and average flutter stability boundary, namely Kf_env and Kf_avr, respectively are determined using the parametric plots shown in Figs. 21 and 22. Then each factor is multiplied by K_all and are used to modify the Regier_env(M), Regier_avr(M), Flutter_env(M) and Flutter_avr(M) as shown in Eqs. (6) and (7).

References

1. MathCad, Version.3.1 Users Guide, MathSoft Inc., 201 Broadway, Cambridge, Mass 02139, 1991. MathCad is registered Trademark of MathSoft Inc.

2. Harris, G., "Flutter Criteria for Preliminary Design," LTV Aerospace Corporation., Vought Aeronautics and Missiles Division, Engineering Report 2-53450/3R-467 under Bureau of Naval Weapons Contract NOW 61-1072C, September 1963.

3. Regier, Arthur A., "The Use of Scaled Dynamic Models in Several Aerospace Vehicle Studies, "*ASME Colloquium on the Use of Models and Scaling in Simulation of Shock and Vibration*, November 19, 1963, Philadelphia, PA.

4. Frueh, Frank J., "A Flutter Design Parameter to Supplement the Regier Number," AIAA Journal. Vol. 2, No. 7, July 1964.

5. Dunn, Henry J. and Doggett, Robert V. Jr., "The Use of Regier Number in the Structural Design with Flutter Constraints," NASA TM 109128, August 1994.

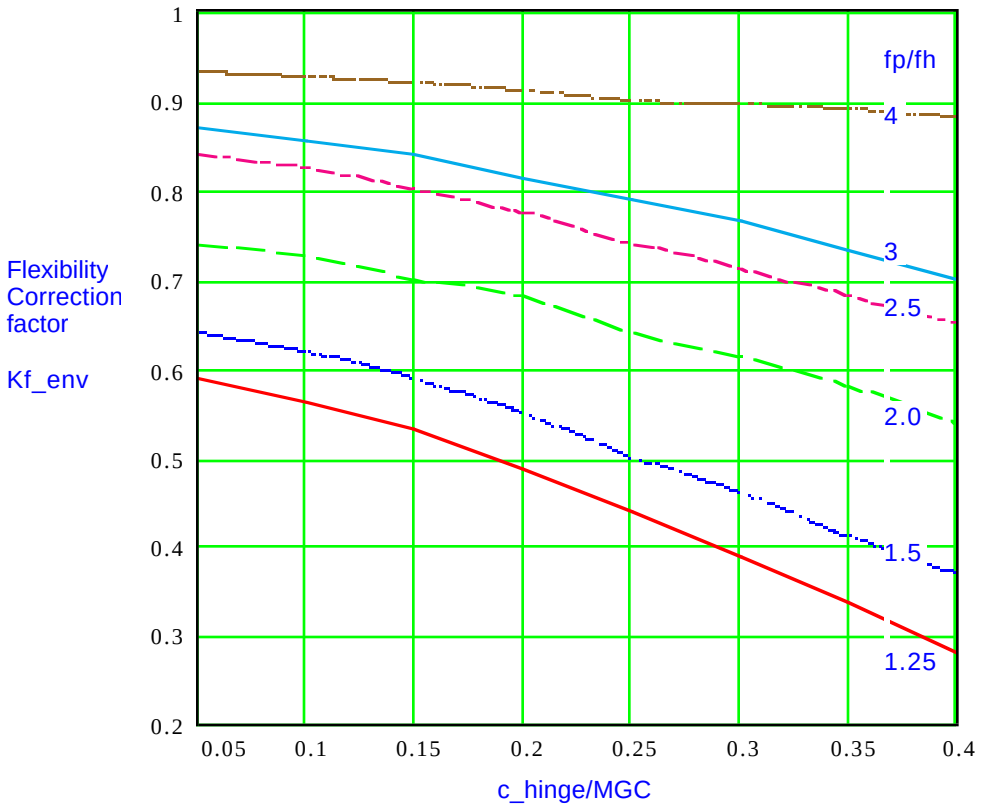

Fig. 21 Wing root flexibility correction factor Kf_env versus elastic axis location.

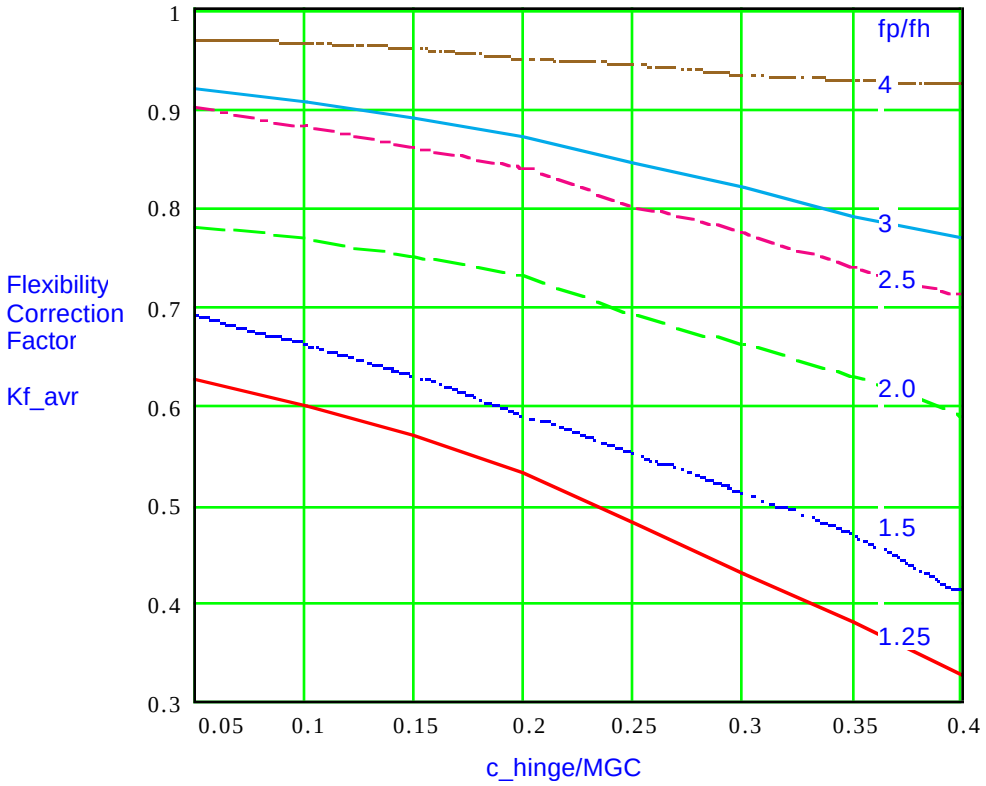

Fig. 22 Wing root flexibility correction factor Kf_avr versus elastic axis location.

6. Liebeck, Robert, H., Page, Mark. A., Rawdon, Blaine K., Scott, Paul W., and Wright Robert A., "Concepts for Advanced Subsonic Transports," NASA CR-4628, McDonnell Douglas Corporation, Long Beach, CA, September 1994.

7. Sweetman Bill and Brown Stuart F, "Megaplanes, the new 800 passenger Jetliners," Popular Mechanics, April 1995, pp. 54-57.

8. Liebeck, Robert, H., Page, Mark. A., " Blended-Wing-Body Configuration Control Document," McDonnell Douglas Corporation, Long Beach, CA, December 1994.

9. Mukhopadhyay, V., "Interactive Flutter Analysis and Parametric Study for Conceptual Wing Design," AIAA paper 95-3943, 1st AIAA Aircraft Engineering, Technology and Operations Congress, Los Angeles, California, September 19-21, 1995.

Availability and distribution

Flutter analysis software for low and medium aspect ratio wing, Version 1.1 is presently available for distribution. It requires MathCad application software for Macintosh or IBM compatible personal computers.

The software is presently being used at the Aerospace Engineering Departments at Virginia Polytechnic Institute and State University. and at the Embry Riddle Aeronautical University, Daytona Beach.

Potential commercial use

Commercial aerospace company, R&D organization and small business, and Universities can use this product during systems analysis and feasibility study in the conceptual airplane wing design stage. The primary objective of a preliminary flutter analysis is to estimate the flutter instability boundary of the flexible cantilever wing along with parametric study of the effect of change in torsional frequency, sweep, mass ratio, aspect ratio, taper ratio, center of gravity, and pitch inertia.

Point of contact

Vivek Mukhopadhyay
Systems Analysis Branch
Aeronautical Systems Analysis Division
MS 248, NASA Langley Research Center
Hampton, Virginia 23681-0001
Phone (804) 864-2835
FAX: (804) 864 -3553
email: v.mukhopadhyay@larc.nasa.gov

For a hard copy of NASA reports

Use World Wide Web NASA Report server at the URL address:

http://techreports.larc.nasa.gov/cgi-bin/NTRS
(Choose NASA Langley and use Key word Mukhopadhyay)

ftp://techreports.larc.nasa.gov/pub/techreports/larc/95/NASA TM 110276.ps.Z

http://techreports.larc.nasa.gov/ltrs/ltrs.html